PROCEEDINGS OF SCIENCE

# New Measurement of the $B_s^0$ Mixing Phase at CDF

**Elisa Pueschel**[*†]
*University of Massachusetts, Amherst*
*E-mail:* elisa.kay.pueschel@cern.ch

The CDF experiment at the Tevatron collider presents improved bounds on the *CP*-violating phase $\beta_s$ and on the decay-width difference $\Delta\Gamma_s$ of the neutral $B_s^0$ meson system. We use 6500 $B_s^0 \to J/\psi\phi$ decays collected by the dimuon trigger and reconstructed in a sample corresponding to 5.2 fb$^{-1}$ of data. Besides exploiting a two-fold increase in statistics with respect to the previous measurement, several improvements have been introduced in the analysis including a fully data-driven flavor-tagging calibration and proper treatment of possible *S*-wave contributions.

*The Xth Nicola Cabibbo International Conference on Heavy Quarks and Leptons,*
*October 11-15, 2010*
*Frascati (Rome) Italy*

[*]Speaker.
[†]on behalf of CDF Collaboration.

 

PoS(HQL 2010)049

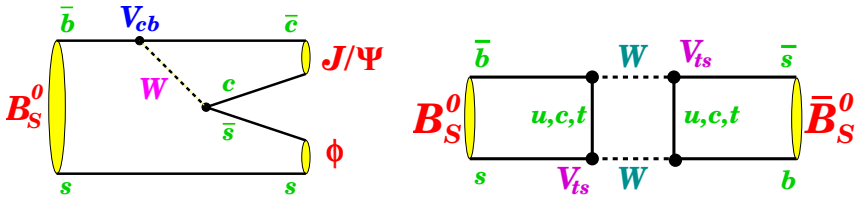


**Figure 1:** The $B_s^0$ meson can decay to $J/\psi\phi$ directly (left), or can mix to a $\bar{B}_s^0$ meson before decaying (right).

## 1. Introduction

The *CP*-violating phase $\beta_s$ is a sensitive probe for the presence of beyond the standard model physics processes in $B_s^0$. This phase can be measured with a time-dependent angular analysis of $B_s^0 \to J\psi\phi$ decays. The measurement is directly analogous to the measurement of the *CP*-violating phase $\beta$ using $B^0 \to J/\psi K_s^0$ decays. In both cases, the neutral meson can either decay directly to the final state, or oscillate into its antiparticle before decaying to the same final state. The mixing process provides an amplitude that interferes with the tree-level amplitude, enabling non-zero *CP*-violation. Feynman diagrams for the tree-level decay and for mixing are shown in Figure 1. The mixing amplitude is dominated by top quark exchange; potentially a heavy beyond the standard model particle, such as a fourth generation *t'* could be exchanged, altering the mixing amplitude and thus the *CP*-violating phase [1].

In the standard model, $\beta_s$ can be expressed in terms of elements of the Cabibbo-Kobayashi-Maskawa matrix. Utilizing the unitary property of the matrix, $\beta_s \equiv arg(-V_{ts}V_{tb}^*/V_{cs}V_{cb}^*)$, with an expected magnitude of $\beta_s \approx 0.02$. A deviation from this expected value would indicate that non-standard model processes contribute to the mixing process.

Previous measurements of $\beta_s$ have shown a non-significant deviation from the standard model expectation for $\beta_s$. An initial measurement at CDF using a 1.35 fb$^{-1}$ data sample found $1.5\sigma$ consistency with the standard model expectation, and increasing the data set to 2.8 fb$^{-1}$ brought the consistency to $1.8\sigma$. The DØ experiment produced an analogous measurement, enabling a combined Tevatron result with a $2.3\sigma$ consistency with the standard model expectation.

In order to quantify the effect of a large *CP* violating phase on the $B_s^0$ meson mixing process, it is necessary to define the relevant mixing observables. The time evolution of the flavor eigenstates $B_s^0$ and $\bar{B}_s^0$ is given by the time dependent Schrodinger equation. Diagonalizing the decay and mass matrices in this equation translates the flavor eigenstates to heavy and light mass eigenstates. The mass and lifetime of the mass eigenstates define the experimentally measurable mass difference or oscillation frequency $\Delta m_s = m_H - m_L$ and lifetime or decay width difference $\Delta\Gamma_s = \Gamma_H - \Gamma_L$, as well as the *CP* phase $\phi_s = arg\frac{-M_{12}}{\Gamma_{12}}$.

It is most reasonable theoretically to expect that a large *CP* violating phase $\phi_s^{NP}$ would be mixing-induced, and thus would alter the *CP* phase $\phi_s$. The standard model expected value for $\phi_s$ is small. Therefore, for large values, $\phi_s^{NP}$ would dominate both $\phi_s$ and $\beta_s$. In this case, with sign conventions included, one can make the approximation $2\beta_s = -\phi_s^{NP} = -\phi_s$.

## 2. Analysis Strategy

The phase $\beta_s$ is measured using $B_s^0/\bar{B}_s^0 \to J/\psi\phi$ decays. Signal events are reconstructed ex-

clusively from decays in which $J/\psi \to \mu^+\mu^-$ and $\phi \to K^+K^-$. An artificial neural network is used to suppress background. In order to extract $\beta_s$, an unbinned maximum likelihood fit is performed, simultaneously fitting to mass, angular distributions, and lifetime.

The decay $B_s^0 \to J/\psi\phi$ is a pseudo-scalar decay to two vector particles, whose angular momenta sum to produce a final state that is an admixture of three angular momenta states, two *CP*-even and one *CP*-odd. An angular analysis using the transversity basis is employed to separate *CP*-odd from *CP*-even contributions [2]. Time dependence is incorporated through a fit to the signal and background lifetimes. The sensitivity to $\beta_s$ is increased by applying flavor tagging algorithms to determine whether the $B_s^0$ meson was produced as a $B_s^0$ or $\bar{B_s^0}$. Examination of the full probability density for $B_s^0$ and $\bar{B_s^0}$ as a function of time and angles demonstrates that incorporation of flavor tagging doubles the number of terms with sensitivity to $\beta_s$.

The likelihood function also folds in the angular efficiency and the calibration of the flavor tagging algorithms. The fit extracts a value for $\beta_s$, and also for correlated parameters of interest: $\Delta\Gamma$, the $B_s^0$ average lifetime $\tau(B_s^0)$, the angular transversity amplitudes $A_0$, $A_{||}$ and $A_\perp$ and the strong phases $\phi_{||}$ and $\phi_\perp$, which are defined by the initial magnitudes of the transversity amplitudes.

Going beyond previous measurements, the most recent measurement takes into account the possibility of signal contamination by $B_s^0 \to J/\psi K^+K^-$ and $B_s^0 \to J/\psi f_0$ decays (*S*-wave contamination). Such decays, if misidentified as signal, will alter the proportion of *CP*-odd to *CP*-even in the final state and bias the measurement of $\beta_s$. This issue is resolved by including terms for non-resonant $K^+K^-$ and $f_0$ in the likelihood fit. Both $K^+K^-$ and $f_0$ are modeled as flat in the narrow $\phi$ mass region used in the measurement, an assumption that was validated by comparison to Monte Carlo line shapes. The $\phi$ resonance is modeled as a relativistic Breit-Wigner. Dependence on the $\phi$ mass was removed by integrating over the $\phi$ mass window. The addition terms associated with the *S*-wave contributions enter the angular terms in the likelihood, resulting in angular components with a purely *S*-wave term, a purely resonant term, and an interference term.

## 3. Data Selection

The measurement was performed using proton and anti-proton collisions at a center of mass energy of 1.96 TeV at the Tevatron. A data set of 5.2 fb$^{-1}$ was used, substantially increasing the statistics from previous measurements. A dimuon trigger was used to collect the data for this measurement. Several features of the CDF detector are key to this analysis. The decay time resolution is approximately 0.1 ps, compared to the lifetimes of *B* mesons, which are on order of 1.5 ps. This resolution is necessary to differentiate successfully between the heavy and light $B_s^0$ mass eigenstates. Particle identification, using $dE/dx$ and time of flight, is important for signal selection and flavor tagging.

An artificial neural network was trained to suppress background. The network was trained on a number of kinematic quantities, including the transverse momentum of tracks and decay particles, and vertex probability for decay particles. The signal mass sidebands were used as the background training sample, and $B_s^0 \to J/\psi\phi$ Monte Carlo was used as the signal training sample. A cut on the neural network output was chosen by optimizing sensitivity on pseudo-experiments, rather than performing a traditional optimization of a figure of merit based on the number of signal and background events.

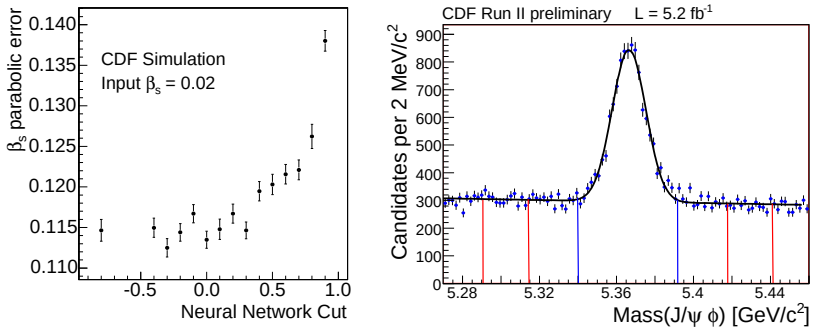


**Figure 2:** Error on $\beta_s$ as a function of simulated neural network output cut (left), $J/\psi\phi$ invariant mass distribution (right).

An ensemble of toys was generated with signal to background ratios corresponding to different neural network output cuts. To demonstrate that the optimal cut does not depend on the generated values of $\beta_s$ and $\Delta\Gamma$, the ensemble was regenerated for several $\beta_s/\Delta\Gamma$ combinations. The errors on $\beta_s$ were examined as a function of signal to background ratio, and the cut that minimized errors was taken. It was observed that for all input values of $\beta_s$, taking a loose cut decreased the errors on $\beta_s$, as shown in Fig. 2. In order to increase sensitivity without introducing unnecessary background, a cut of 0.2 was used, corresponding to approximately 6500 signal events. The $J/\psi\phi$ invariant mass spectrum is shown in Fig. 2.

## 4. Flavor Tagging Calibration

The flavor tagging algorithms used for this measurement were not developed on $B_s^0 \to J/\psi\phi$ decays, and thus needed to be calibrated to accurately predict the tagging power in this data sample. Two tagging algorithms were used: the opposite side tagger and the same side kaon tagger. At the Tevatron, $b$ quarks are produced in $b\bar{b}$ pairs. The tracks produced in association with the reconstructed $B$ meson are referred to as same-side, and those resulting from the fragmentation of the non-reconstructed member of the $b\bar{b}$ pair are referred to as opposite side. Determining the flavor of the opposite side $b$ quark allows the flavor of the same side quark can be inferred, in the case of opposite side tagging. In the case of same side tagging, the charge of the associated track is determined by whether the track was produced in association with a $B_s^0$ or $\bar{B}_s^0$ meson.

The opposite side fragmentation behavior is independent of the reconstructed meson species, which makes it possible to calibrate the opposite side tagger on $B^+ \to J/\psi K^+$ decays. These decays are self-tagging; a $K^+$ must come from a $B^+$ decay and a $K^-$ must come from a $B^-$ decay. The measured dilution, a measure of how likely a tag decision is to be correct, can be compared to the dilution predicted by the algorithm to obtain a scale factor. The comparison of measured to predicted dilution for $B^+$ events is shown in Fig. 3. The dilution scale factors are consistent with unity for both $B^+$ and $B^-$ events. The opposite side tagging power, defined as the efficiency multiplied with the squared dilution, is $1.2\pm0.2\%$.

The same side kaon tagger must be calibrated on a $B_s^0$ sample, because the type of track produced in association with the reconstructed meson is dependent on the meson species. The

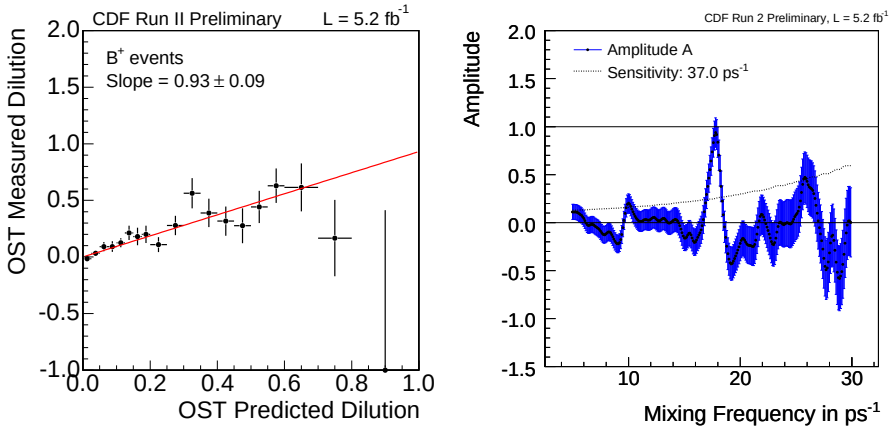


**Figure 3:** Measured versus predicted tagging dilution for $B^+ \to J/\psi K^+$ (left), amplitude scan of $B_s^0$ mixing frequency (right).

measured versus predicted dilution was determined by remeasuring $B_s^0$ mixing on the full 5.2 fb$^{-1}$ data set, using $B_s^0 \to D_s^- \pi^+$ and $B_s^0 \to D_s^-(3\pi)^+$ decays. For an amplitude scan of the mixing frequency, the probability is normalized such that the amplitude is unity at the true value of $\Delta m_s$ in the absence of a dilution scale factor. The scale factor is accounted for by performing the amplitude scan and checking the maximum measured amplitude. The amplitude scan of $\Delta m_s$ is shown in Fig. 3. The maximum amplitude or dilution scale factor is consistent with unity, and value of $\Delta m_s$ for which it occurs is consistent with the world average at $\Delta m_s$=17.79$\pm$0.07 ps$^{-1}$($stat$). The same side kaon tagger has a much higher dilution than the opposite side tagger, with a tagging power of 3.1$\pm$1.4%.

## 5. Results

Fit projections were used to check the fit performance for the proper time distribution and the transversity angle distributions. The fit projection for the proper time is shown in Fig. 4. The lifetime distributions are different for the heavy and light $B_s^0$ mass eigenstates, enabling the world's best measurements of $\Delta\Gamma$ and the $B_s^0$ average lifetime. Fit projections for the proper time distribution and for the three transversity angles show good agreement between the fit and the data distributions.

The likelihood shows biases (particularly for $\beta_s$) and non-Gaussian behaviors when $\beta_s$ is allowed to float in the fit. When $\beta_s$ is fixed to zero, the likelihood is well-behaved, making it possible to quote values for the remaining parameters of interest. The results are the following:

$$
\begin{aligned}
c\tau_s &= 458.7 \pm 7.5\ (\text{stat.})\ \mu\text{m} \pm 3.6\ (\text{syst.})\ \mu\text{m} \\
\Delta\Gamma &= 0.075 \pm 0.035\ (\text{stat.})\ ps^{-1} \pm 0.010\ (\text{syst.})\ ps^{-1} \\
|A_{\parallel}(0)|^2 &= 0.231 \pm 0.014\ (\text{stat}) \pm 0.015\ (\text{stat}) \\
|A_0(0)|^2 &= 0.524 \pm 0.013\ (\text{stat}) \pm 0.015\ (\text{syst}) \\
\delta_{\perp} &= 2.95 \pm 0.65\ (\text{stat}) \pm 0.07\ (\text{syst}).
\end{aligned}
$$

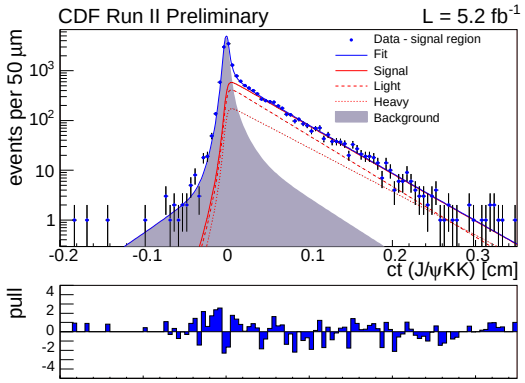


**Figure 4:** The $B_s^0$ meson's proper time fit projection. The lifetime distributions for the heavy and light mass eigenstates are denoted by the dashed red lines.

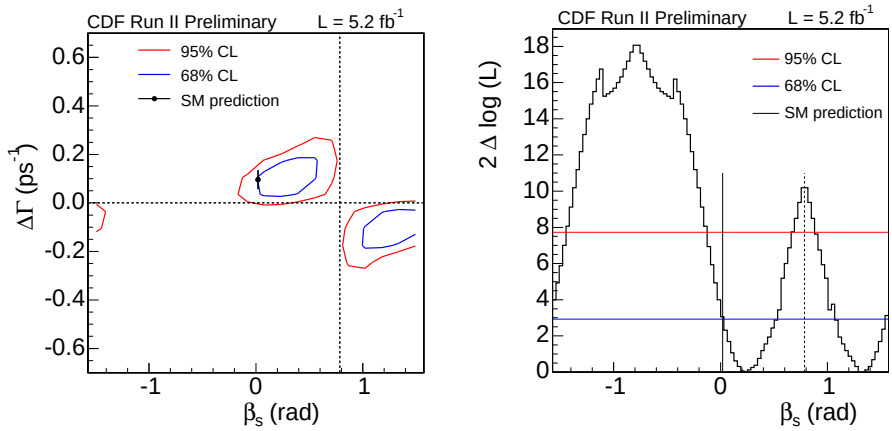


**Figure 5:** Confidence regions in the $\beta_s - \Delta\Gamma$ plane (left) and $\beta_s$ (right).

For the fit with $\beta_s$ floating, a profile likelihood ordering technique was used to guarantee coverage at the 68% and 95% confidence levels. The final contour in the $\beta_s - \Delta\Gamma$ plane is shown in the left plot in Fig. 5. The p-value at the standard model point was calculated to be 44%, indicating $0.8\sigma$ consistency with the standard model expectation. This measurement is more consistent with the standard model expectation than previous measurements have been. In comparison to the previous measurement on 2.8 fb$^{-1}$, shown in Fig. 6, the size of the contour has decreased significantly with increased statistics and analysis improvements. Good consistency exists between the two measurements.

The right plot in Fig. 5 shows the one dimensional $\beta_s$ confidence interval. The p-value at the standard model point for this case is 31%. At the 68% confidence level, $\beta_s$ is in the interval [0.28, 0.52] $\cup$ [1.08, 1.55].

The impact of non-resonant $K^+K^-$ and $f_0$ contributions on the final result was assessed in several ways. A likelihood scan of the $S$-wave fraction was performed. The fraction found to be less than 7% at the 95% confidence level. The $K^+K^-$ invariant mass spectrum was fit in a wide mass window. Good consistency with the data was achieved without including $K^+K^-$ or $f_0$ in the

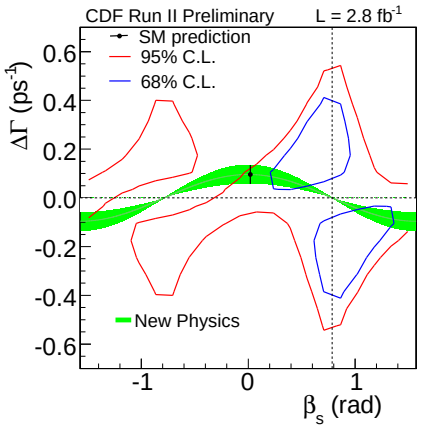


**Figure 6:** Confidence region in the $\beta_s - \Delta\Gamma$ plane for 2.8 fb$^{-1}$ result.

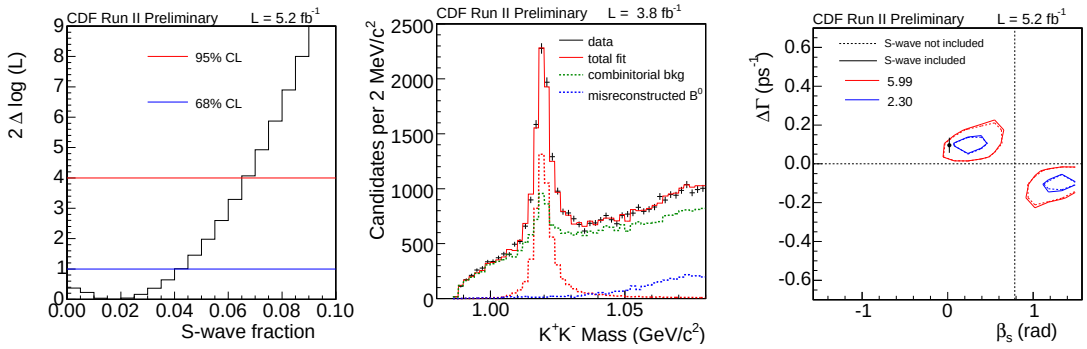


**Figure 7:** Likelihood scan of *S*-wave fraction (left), fit to $K^+K^-$ invariant mass spectrum (middle), $\beta_s - \Delta\Gamma$ contours with and without the *S*-wave contributions included in fit (right).

fit. Lastly, a $\beta_s - \Delta\Gamma$ contour was made with and without the *S*-wave included in the likelihood. The effect of removing the *S*-wave terms from the likelihood was not significant. All three checks are shown in Fig. 7.

## 6. Conclusions

A measurement of the *CP*-violating phase $\beta_s$ has been performed on 5.2 fb$^{-1}$ of data by the CDF experiment. The errors on $\beta_s$ have decreased significantly from previous measurements, and consistency with the standard model expectation has improved. CDF is expected to double its data set before the end of its running period, allowing an even more competitive measurement of this important parameter.

## References

[1] I. Dunietz, R. Fleischer and U. Nierste, Phys. Rev. D **63** (2001) 114015.

[2] A. S. Dighe, I. Dunietz and R. Fleischer, Eur. Phys. J. C **6** (1999) 647.

[3] T. Aaltonen et. al [CDF collaboration], CDF public note 10206 (2010).